SIAM J. SCI. COMPUT.
Vol. 36, No. 4, pp. B684–B707

DISCONTINUOUS SPECTRAL ELEMENT METHODS FOR TIME- AND SPACE-FRACTIONAL ADVECTION EQUATIONS*

MOHSEN ZAYERNOURI† AND GEORGE EM KARNIADAKIS‡

Abstract. We develop spectral element methods for a time- and space-fractional advection equation of the form ${}_0\mathcal{D}_t^\tau u(x,t) + \theta\ {}_0\mathcal{D}_x^\nu u(x,t) = f(x,t)$, of order $\tau \in (0,1]$, $\nu \in (0,1)$, subject to Dirichlet initial/boundary conditions. We present two spectrally accurate and efficient methods for *global* discretization of both temporal and spatial terms, instead of employing traditional low-order time-integration methods. To this end, we first develop a Petrov–Galerkin in time and discontinuous Galerkin in space (PG-DG) method, where we carry out the time-integration using a single time-domain spectral method (SM), and we perform the spatial discretization using the discontinuous spectral/*hp* element method (DSEM). This scheme also leads to a more efficient time-integration when the time-derivative is integer-order, i.e., $\tau = 1$. We develop the SM-DSEM scheme based on a new spectral theory for fractional Sturm–Liouville problems (FSLPs), recently presented in *J. Comput. Phys.*, 47 (2013), pp. 2108–2131. We choose the corresponding space-time bases from the span of tensor product of the introduced eigenfunctions. Specifically, we employ the eigenfunctions of the FSLP of *first* kind (FSLP-I), called *Jacobi polyfractonomial*s, as temporal bases. We also employ the corresponding *asymptotic* eigensolutions to FSLP-I, which are Jacobi polynomials, as the spatial basis. Next, we construct a different test function space, defined as the span of tensor product of polyfractonomial eigenfunctions of the FSLP of *second* kind (FSLP-II), as the temporal test functions and the corresponding *asymptotic* eigensolutions to FSLP-II as the spatial ones. Subsequently, we extend PG-DG to a DG-DG scheme employing the DG method in both time and space. In this scheme, both time-integration and spatial discretization are performed in a DSEM fashion (DSEM-DSEM). Our numerical tests confirm the expected spectral/algebraic convergence, respectively, in corresponding *p*- and *h*-refinements in various test cases and show a four-order of magnitude speed-up compared to finite-difference discretizations.

Key words. fractional PDEs, Jacobi polyfractonomials, fractional basis functions, spectral convergence

AMS subject classifications. 34L10, 58C40, 65M70, 65M60

DOI. 10.1137/130940967

1. Introduction.

Fractional calculus is a unifying theory that generalizes the notion of the standard integer-order differentiation and integration to any real-valued order [28, 6, 30]. Particularly, for instance, it has been shown that the wall-friction through the fluid boundary layer exhibits some cumulative memory effects, giving rise to fractional partial derivatives in Navier–Stokes equations [7, 17, 36]. The notion of fractional differential operators has been rapidly extended to many fractional partial differential equations (FPDEs) such as the fractional Burgers' equation [35], the fractional Fokker–Planck equation [2], and the fractional advection-diffusion equation [13]. However, the extension of existing numerical methods, developed for integer-order PDEs (see e.g., [11, 22, 14, 43, 16] and references therein) to their corresponding FPDEs is not a straightforward task. It is mainly because of the *nonlocal* nature

*Submitted to the journal's Computational Methods in Science and Engineering section October 11, 2013; accepted for publication (in revised form) April 30, 2014; published electronically August 5, 2014. This work was supported by the Collaboratory on Mathematics for Mesoscopic Modeling of Materials (CM4) at PNNL, funded by the Department of Energy, by OSD/MURI, and by NSF/DMS.
http://www.siam.org/journals/sisc/36-4/94096.html

†Division of Applied Mathematics, Brown University, Providence, RI 02912 (mohsen_zayernouri@brown.edu).

‡Corresponding author. Division of Applied Mathematics, Brown University, Providence, RI 02912 (george_karniadakis@brown.edu).

and long-range *history*-dependence of fractional differential operators. However, the development of numerical schemes in this area has received enormous attention and has undergone a fast evolution in recent years. Most of numerical methods developed for integer-order PDEs have been applied to FPDEs; methods such as finite difference methods (FDM), spectral methods (SM), and finite or spectral element methods (FEM, SEM).

The implementation of FDM approaches (see, e.g., [9, 21, 37, 4]) is relatively easy; however, the challenging issue in FDM is that the convergence is *algebraic* and the accuracy is limited. Moreover, FDM suffers from the heavy cost of computing the long-range memory since FDM is inherently a *local* approach, whereas fractional derivatives are essentially *global* (nonlocal). This fact would suggest global schemes such as SMs may be more appropriate tools for discretizing FPDEs.

The early works in SM were developed in [35, 3, 31] employing collocation approaches. The idea of collocation was later adopted by Khader [18], who proposed a Chebyshev collocation method for the discretization of the space-fractional diffusion equation. More recently, Khader and Hendy [19] developed a Legendre pseudospectral method for fractional-order delay differential equations. The aforementioned schemes are relatively easy to implement; however, their performance has not been tested rigorously or systematically and only limited cases have been examined. The first fundamental work on SMs for FPDEs was done by Li and Xu [23, 24] and was based on the early work of Fix and Roop [10]. They developed a time-space SM for time-fractional diffusion equation, where the spatial term is integer-order, with exponential convergence. In this scheme, the corresponding stiffness and mass matrices, however, are dense and gradually become ill-conditioned when the fractional order tends to small values. Hence, due to the nature of single-domain SMs, carrying out long-time and/or adaptive integration using such an SM becomes prohibited. Moreover, we note that the expected fast convergence in SMs is achieved only when the solution belongs to higher Sobolev spaces and possesses high regularity. This motivates employing domain decomposition and developing proper FEMs in addition to SEMs in an efficient form.

Unlike the great effort put into developing FDM and the considerable work done on SM schemes, very little attention has been given to developing rigorous high-order FEM and SEM methods. Fix and Roop [10] developed the first theoretical framework for the least-square FEM approximation of a fractional-order differential equation, where optimal error estimates are proven for piecewise linear elements. However, Roop [33] later showed that the main hurdle to overcome in the FEM is the nonlocal nature of the fractional operator, which leads to large dense matrices; he showed that even the construction of such matrices presents difficulties. Among other rigoours works, McLean and Mustapha [26] developed a piecewise-constant discontinuous Galerkin (DG) method for the time-discretization of a subdiffusion equation. A Chebyshev-SEM for fractional-order transport was adopted by Hanert [12], and later on, the idea of the least-square FEM was extended to SEMs by Carella [5]. Recently, Deng and Hesthevan [8] and Xu and Hesthaven [39] developed local DG methods for solving space-fractional diffusion and advection-diffusion problems with optimal accuracy.

In our earlier study in [41], we developed efficient and highly accurate Petrov–Galerkin (PG) spectral and DG for fractional ODEs of the form ${}_0\mathcal{D}_t^\tau u(t) = f(t)$ and ${}_t\mathcal{D}_T^\tau u(t) = f(t)$, $\tau \in (0,1)$, subject to Dirichlet initial conditions. The goal of the present study is to generalize the aforementioned schemes to linear hyperbolic FPDEs, where the corresponding temporal and spatial stiffness/mass matrices coexist. The main contribution of this paper is the development of highly accurate

and efficient methods for time- and space- fractional advection equation (TSFAE) of the form ${}_0\mathcal{D}_t^\tau u(x,t) + \theta\ {}_0\mathcal{D}_x^\nu u(x,t) = f(x,t)$ of order $\tau \in (0,1]$, $\nu \in (0,1)$. We accomplish this following the spectral theory on the fractional Sturm–Liouville eigenproblem, recently developed in [40], where the corresponding eigenfunctions, called *Jacobi polyfractonomial*s, are employed as basis and test functions.

The TSFAE problem is of physical and mathematical importance. From the viewpoint of transport kinetics, this equation governs the PDF of the continuous-time random walk limit processes, known as $\tau\&\nu$-stable Lévy processes with strictly positive jumps and waiting times when the spatial order $\nu \in (0,1)$ [27]. In fluid mechanics, the aforementioned equation when $\tau = 1/2$ and $\nu \to 1$ has been shown to be equivalent to the governing equations in Stokes' first and second problems after performing a proper change of variable through Laplace transform [20]. From the mathematical development point of view, our approach is analogous to the first DG method, developed in 1973 [32] for time-independent linear advection equations that paved the way for further development of DG schemes for other PDEs. The present study provides a suitable platform for further development of PG-DG methods for higher-order FPDEs such as fractional wave or advection-diffusion equation. Here in this study, the major feature of our schemes is the *global* and multielement discretization of the temporal term, in addition to the spatial term, rather than utilizing traditional low-order time-integration methods, particularly when $\tau = 1$.

We first develop a PG in time and DG in space (PG-DG) method, where we carry out the time-integration using an SM-type discretization, and we perform the spatial discretization using the discontinuous spectral/*hp* element method (DSEM). This scheme is in contrast to the traditional approaches (e.g., see [25]) which treat the temporal term using FDM and discretize the spatial term by SM. In fact, in such mixed FDM-SM schemes, the high-order spatial descretization can be easily polluted by the low accuracy of the time-integration. Here, we develop the SM-DSEM scheme based on a new spectral theory for fractional Sturm–Liouville problems (FSLPs), introduced in [40], which provides proper spaces of basis and test functions. Subsequently, we extend the PG-DG to a DG-DG scheme, in which both time-integration and spatial discretization are performed in an *hp*-element fashion (DSEM-DSEM). In contrast to common FEM/SEM methods, in which the construction of the corresponding mass and stiffness matrices is challenging (see, e.g., [33]), all the aforementioned matrices in our methods are constructed *exactly* and *efficiently*.

The organization of the paper is as follows. In section 2, we present the notation and the problem definition. In section 3, we introduce the first method, i.e., PG-DG employing SM-DSEM in time and space, in addition to the corresponding spaces of the basis and test functions. In section 4, we consider a special case, where the temporal-order $\tau = 1$ in SM-DSEM, and we introduce this method as a spectrally accurate time-integration scheme for problems of form $\partial u/\partial t = F(u;x,t)$. In section 5, we extend this scheme to the second method, called DG-DG, by employing DSEM-DSEM in both time and space, and we demonstrate its performance in long-time integration. We end the paper with a summary and discussion in section 6, and Appendix A includes the derivation of the SM-DSEM.

2. Problem definition. We consider the following TSFAE:

$$
\begin{aligned}
{}_0\mathcal{D}_t^\tau u(x,t) + \theta\ {}_0\mathcal{D}_x^\nu u(x,t) &= f(x,t), \quad (x,t) \in [0,L] \times [0,T], \\
u(x,0) &= g(x), \\
u(0,t) &= h(t),
\end{aligned}
\tag{2.1}
$$

where $\theta > 0$, $g \in C[0, L]$, and $h \in C[0, T]$, such that $g(0) = h(0) = 0$. Moreover, denote by ${}_0\mathcal{D}_t^\tau u(x,t)$ the left-sided Reimann–Liouville time-fractional derivative of order $\tau \in (0, 1]$ following [30], defined as

$$ {}_0\mathcal{D}_t^\tau u(x,t) = \frac{1}{\Gamma(1-\tau)} \frac{\partial}{\partial t} \int_0^t \frac{u(x,s)}{(t-s)^\tau}\, ds, \quad t > 0, \quad x \in [0, L], \tag{2.2}$$

in which Γ represents the Euler gamma function. In (2.2), as $\nu \to 1$, the *global* (nonlocal) operator ${}_0\mathcal{D}_t^\tau u(x,t) \to \partial u(x,t)/\partial t$, recovering the *local* first-order partial derivative with respect to t. Also, ${}_0\mathcal{D}_x^\nu u(x,t)$ denotes the left-sided Reimann–Liouville space-fractional derivative of order $\nu \in (0, 1)$, defined as

$$ {}_0\mathcal{D}_x^\nu u(x,t) = \frac{1}{\Gamma(1-\nu)} \frac{\partial}{\partial x} \int_0^x \frac{u(z,t)}{(x-z)^\nu}\, dz, \quad x > 0, \quad t \in [0, T]. \tag{2.3}$$

We could also define the fractional derivatives in (2.1) to be of Caputo fractional derivative sense i.e., ${}_0^C\mathcal{D}_t^\tau$ and ${}_0^C\mathcal{D}_x^\nu$, respectively, defined as

$$ {}_0^C\mathcal{D}_t^\tau u(x,t) = \frac{1}{\Gamma(1-\tau)} \int_0^t \frac{\partial u(x,s)/\partial s}{(t-s)^\tau}\, ds, \quad t > 0, \quad x \in [0, L], \tag{2.4}$$

and

$$ {}_0^C\mathcal{D}_x^\nu u(x,t) = \frac{1}{\Gamma(1-\nu)} \int_0^x \frac{\partial u(z,t)/\partial z}{(x-z)^\nu}\, dz, \quad x > 0, \quad t \in [0, T]. \tag{2.5}$$

These fractional operators are defined in fact by interchanging the order of the integration and differentiation in (2.2) and (2.3). However, the two definitions are closely linked by the following relationships:

$$ {}_0\mathcal{D}_t^\tau u(x,t) = \frac{g(x)}{\Gamma(1-\tau)\, t^\tau} + {}_0^C\mathcal{D}_t^\tau u(x,t) \tag{2.6}$$

and

$$ {}_0\mathcal{D}_x^\nu u(x,t) = \frac{h(t)}{\Gamma(1-\nu)\, x^\nu} + {}_0^C\mathcal{D}_x^\nu u(x,t), \tag{2.7}$$

By virtue of (2.6) and (2.7), the TSFAE (2.1) becomes identical to the corresponding problem with the Caputo fractional derivatives when $g(x) = h(t) = 0$. Without loss of generality, we consider (2.1) subject to homogeneous Dirichlet initial and boundary conditions in this study. Moreover, we note that when the aforementioned fractional derivatives apply to a *univariate* function, the corresponding partial derivative is replaced by an *ordinary* derivative one.

3. PG-DG method: SM-in-time and DSEM-in-space. We develop a PG-DG method for (2.1), where the time-fractional order $\tau \in (0, 1]$ and space-fractional order $\nu \in (0, 1)$, subject to homogeneous Dirichlet initial/boundary conditions. Here, we aim, rather than utilizing traditional low-order time-integrators such as FDM when $\tau \in (0, 1)$ or Adams families when $\tau = 1$, to treat the temporal term $\forall \tau \in (0, 1]$ globally by employing an SM in the single time-domain $[0, T]$. Moreover, we perform the spatial discretization by a DSEM. In the SM-DSEM scheme, we partition the computational domain into N_{el} nonoverlapping *space-time* elements, $\Omega_e = [x_{e-1/2}, x_{e+1/2}] \times [0, T]$, such that $\cup_{e=1}^{N_{el}} \Omega_e = [0, L] \times [0, T]$. In SM-DSEM, the new eigensolutions, introduced in [40], yield new sets of *basis* and *test* functions, properly suited for our PG framework.

3.1. Basis functions. In SM-DSEM, we represent the solution in each space-time element Ω_e in terms of special basis functions, constructed as the tensor product of the eigenfunctions in the following manner. We first recall the following *Jacobi polyfractonomials*, obtained as the eigenfunctions of the FSLP of first kind explicitly in [40] as

$$ {}^{(1)}\mathcal{P}_n^{\alpha,\beta,\mu}(x) = (1+x)^{-\beta+\mu-1} P_{n-1}^{\alpha-\mu+1,-\beta+\mu-1}(x), \quad x \in [-1,1], \tag{3.1}$$

where $P_{n-1}^{\alpha-\mu+1,-\beta+\mu-1}(x)$ are the standard Jacobi polynomials in which $\mu \in (0,1)$, $-1 \le \alpha < 2-\mu$, and $-1 \le \beta < \mu - 1$. Particularly, ${}^{(1)}\mathcal{P}_n^{\alpha,\beta,\mu}(x)$ represent the eigenfunctions of the *singular* FSLP of first kind (SFSLP-I) when $\alpha \neq -1$ and $\beta \neq -1$; otherwise ${}^{(1)}\mathcal{P}_n^{\mu}(x) \equiv {}^{(1)}\mathcal{P}_n^{-1,-1,\mu}(x)$ denote the eigenfunctions of the *regular* FSLP of first kind (RFSLP-I). The eigenfunctions (3.1) are the baseline of our space-time basis construction.

To define the *spatial* basis in the interval $[x_{e-1/2}, x_{e+1/2}]$, let the fractional power of the multiplier term in (3.1) $(-\beta+\mu-1) \to 0$; then ${}^{(1)}\mathcal{P}_n^{\alpha,\beta,\mu}(x) \to P_{n-1}^{\alpha-\mu+1,0}(x)$, where $\alpha-\mu+1 = \eta \in (0,1)$, since $-1 \le \alpha < 2-\mu$ and $-1 \le \beta < \mu - 1$, recalled from [40]. Hence, through an affine mapping from $[-1,1]$ to $[x_{e-1/2}, x_{e+1/2}]$, we define the spatial basis as

$$ \widetilde{P}_m^{\eta,0}(x^e), \ m = 0,1,2,\ldots, \quad x^e \in [x_{e-1/2}, x_{e+1/2}], \tag{3.2}$$

which are Jacobi polynomials associated with the parameters η and 0.

In order to define the *temporal* basis in the interval $[0,T]$, we recall that the regular $\{{}^{(1)}\mathcal{P}_n^{\mu}(x)\}_{n=1}^N$ and singular $\{{}^{(1)}\mathcal{P}_n^{\alpha,\beta,\mu}(x)\}_{n=1}^N$ sets (for some $N \in \mathbb{N}$) have identical approximating properties when $\alpha = \beta$. Hence, by choosing $\alpha = \beta = -1$ and through the affine mapping $x(t) = 2t/T - 1$, from the standard interval $[-1,1]$ to $[0,T]$ we define our temporal basis as

$$ {}^{(1)}\widetilde{\mathcal{P}}_n^{\mu}(t) = \left(\frac{2}{T}\right)^{\mu} t^{\mu} P_{n-1}^{-\mu,\mu}(x(t)), \ n = 1,2,\ldots, \quad t \in [0,T], \tag{3.3}$$

known as a *shifted* Jacobi polyfractonomial of fractional order $(n-1+\mu)$. Now, having defined the spatial and temporal functions in (3.2) and (3.3), we construct the space-time trial (basis) space V^e as

$$ V^e \equiv span\{\widetilde{P}_m^{\eta,0}(x^e)\ {}^{(1)}\widetilde{\mathcal{P}}_n^{\mu}(t) : m = 0,1,\ldots,M, n = 1,2,\ldots,N\}, \tag{3.4}$$

where we shall approximate the solution to (2.1) in terms of a linear combination of elements in V^e. The corresponding space-time basis functions are then *discontinuous* in space at the interfaces of elements Ω_e, $e = 1,2,\ldots,N_{el}$, while they satisfy the homogeneous initial condition in the single time-domain.We note that the corresponding *nodal* representation of (3.3) has been recently employed in developing fractional spectral collocation methods for fractional ODEs/PDEs [42].

3.1.1. Fractional derivatives of the bases. The following lemma is useful to obtain the space-fractional derivative of the spatial basis $\widetilde{P}_m^{\eta,0}(\,x^e\,)$.

LEMMA 3.1 (see [1]). *For $\mu > 0$, $\alpha > -1$, $\beta > -1$, and $\forall x \in [-1,1]$*

$$ (1+x)^{\beta+\mu} \frac{P_m^{\alpha-\mu,\beta+\mu}(x)}{P_m^{\alpha-\mu,\beta+\mu}(-1)} = \frac{\Gamma(\beta+\mu+1)}{\Gamma(\beta+1)\Gamma(\mu)P_m^{\alpha,\beta}(-1)} \int_{-1}^{x} \frac{(1+s)^{\beta}\ P_m^{\alpha,\beta}(s)}{(x-s)^{1-\mu}} ds. \tag{3.5}$$

By the definition of the left-sided Riemann–Liouville integral ${}_{-1}\mathcal{I}_x^{\mu}$ (see, e.g., [30]) and evaluating the special end-values $P_m^{\alpha-\mu,\beta+\mu}(-1)$ and $P_m^{\alpha,\beta}(-1)$, we can rewrite (3.5) as

$$ {}_{-1}\mathcal{I}_x^{\mu}\Big\{(1+x)^{\beta}P_m^{\alpha,\beta}(x)\Big\} = \frac{\Gamma(m+\beta+1)}{\Gamma(m+\beta+\mu+1)}(1+x)^{\beta+\mu}\,P_m^{\alpha-\mu,\beta+\mu}(x). \tag{3.6}$$

Now, by taking the fractional derivative ${}_{-1}\mathcal{D}_x^{\mu}$ on both sides of (3.6) when $\beta=-\mu$ we obtain

$$ {}_{-1}\mathcal{D}_x^{\mu}\Big\{P_m^{\alpha-\mu,0}(x)\Big\} = \frac{\Gamma(m+1)}{\Gamma(m-\mu+1)}(1+x)^{-\mu}P_m^{\alpha,\,-\mu}(x). \tag{3.7}$$

Moreover, from the properties of the eigensolutions in [40], the left-sided Riemann–Liouville fractional derivative of (3.3) is given as

$$ {}_0\mathcal{D}_t{}^{\mu}\Big({}^{(1)}\widetilde{\mathcal{P}}_n{}^{\mu}(t)\Big) = \left(\frac{2}{T}\right)^{\mu}\frac{\Gamma(n+\mu)}{\Gamma(n)}P_{n-1}(x(t)), \tag{3.8}$$

stating that the μth order fractional derivative of such fractal (nonpolynomial) basis functions of order $(n-1+\mu)$ is a standard Legendre polynomial of integer-order $(n-1)$.

3.2. Test functions. In order to construct the space of test functions, we recall the following Jacobi polyfractonomials, introduced as the eigensolutions of the FSLP of the *second* kind, obtained explicitly as

$$ {}^{(2)}\mathcal{P}_n^{\alpha,\beta,\mu}(x) = (1-x)^{-\alpha+\mu-1}P_{n-1}^{-\alpha+\mu-1,\,\beta-\mu+1}(x), \quad x\in[-1,1], \tag{3.9}$$

in [40], where $-1<\alpha<\mu-1$ and $-1<\beta<2-\mu$, and $\mu\in(0,1)$. Particularly ${}^{(2)}\mathcal{P}_n^{\alpha,\beta,\mu}(x)$ denote the eigenfunctions of the *singular* FSLP of second kind (SFSLP-II) when $\alpha\neq-1$ and $\beta\neq-1$, and ${}^{(2)}\mathcal{P}_n{}^{\mu}(x)\equiv{}^{(2)}\mathcal{P}_n^{-1,-1,\mu}(x)$ denote the eigenfunctions of the *regular* FSLP of first kind (RFSLP-II). In a similar fashion, we employ the eigenfunctions (3.9) as the baseline of construction for our space-time test functions.

To define the *spatial* test functions in the interval $[x_{e-1/2},x_{e+1/2}]$, we set the power of the fractional multiplier in (3.9) $(-\alpha+\mu-1)\to0$, then ${}^{(2)}\mathcal{P}_n^{\alpha,\beta,\mu}(x)\to P_{n-1}^{0,\beta-\mu+1}(x)$, where $\beta-\mu+1=\chi\in(0,1)$. Hence, we define the spatial basis as

$$ \widetilde{P}_i^{\,0,\chi}(x^e),\ i=0,1,2,\ldots, \quad x^e\in[x_{e-1/2},x_{e+1/2}], \tag{3.10}$$

which are Jacobi polynomials associated with the parameters 0 and χ. We also define the *temporal* basis in the interval $[0,T]$ by choosing $\alpha=\beta=-1$ in (3.9) and mapping from the standard interval $[-1,1]$ to $[0,T]$ as

$$ {}^{(2)}\widetilde{\mathcal{P}}_j{}^{\mu}(t) = \left(\frac{2}{T}\right)^{\mu}(T-t)^{\mu}P_{j-1}^{\mu,\,-\mu}(x(t)),\ j=1,2,\ldots, \quad t\in[0,T]. \tag{3.11}$$

Now, having defined the spatial and temporal functions in (3.10) and (3.11), we construct the space-time test space $\mathcal{V}^e$ as

$$ \mathcal{V}^e \equiv span\{\widetilde{P}_i^{\,0,\chi}(x^e)\ {}^{(2)}\widetilde{\mathcal{P}}_j{}^{\mu}(t) : i=0,1,\ldots,M, j=1,2,\ldots,N\}, \tag{3.12}$$

where we test the problem (2.1) against the elements in $\mathcal{V}^e$.

3.2.1. Fractional derivatives of the test functions. We use the following lemma to calculate the space-fractional derivative of the spatial test functions $\widetilde{P}_i^{0,\chi}(x^e)$.

LEMMA 3.2 (see [1]). *For $\mu > 0$, $\alpha > -1$, $\beta > -1$, and $\forall x \in [-1, 1]$*

$$(1-x)^{\alpha+\mu}\,\frac{P_i^{\alpha+\mu,\beta-\mu}(x)}{P_i^{\alpha+\mu,\beta-\mu}(+1)} = \frac{\Gamma(\alpha+\mu+1)}{\Gamma(\alpha+1)\Gamma(\mu)P_i^{\alpha,\beta}(+1)}\int_x^1 \frac{(1-s)^\alpha\ P_i^{\alpha,\beta}(s)}{(s-x)^{1-\mu}}ds. \tag{3.13}$$

Once again by the definition of the right-sided Riemann–Liouville integral ${}_x\mathcal{I}_1^\mu$ (see, e.g., [30]) and evaluating the special end-values $P_i^{\alpha-\mu,\beta+\mu}(+1)$ and $P_i^{\alpha,\beta}(+1)$, we can recast (3.13) as

$${}_x\mathcal{I}_1^\mu\Big\{(1-x)^\alpha P_i^{\alpha,\beta}(x)\Big\} = \frac{\Gamma(i+\alpha+1)}{\Gamma(i+\alpha+\mu+1)}(1-x)^{\alpha+\mu}P_i^{\alpha+\mu,\beta-\mu}(x). \tag{3.14}$$

In a similar fashion, by taking the fractional derivative ${}_x\mathcal{D}_{-1}^\mu$ on both sides of (3.14) when $\alpha = -\mu$ we obtain

$${}_x\mathcal{D}_1^\mu\Big\{P_i^{0,\beta-\mu}(x)\Big\} = \frac{\Gamma(i+1)}{\Gamma(i-\mu+1)}(1-x)^{-\mu}P_i^{-\mu,\beta}(x). \tag{3.15}$$

The relations (3.7) and (3.15) are useful in computing the corresponding spatial *stiffness* matrix in the discontinuous SM-DSEM.

Next, following [40], the right-sided Riemann–Liouville fractional derivative of (3.11) is obtained as

$${}_t\mathcal{D}_T^\mu\left({}^{(2)}\widetilde{\mathcal{P}}_j^{\,\mu}(t)\right) = \left(\frac{2}{T}\right)^\mu\ \frac{\Gamma(j+\mu)}{\Gamma(j)}P_{j-1}(x(t)). \tag{3.16}$$

The relations (3.8) and (3.16) will be employed in computing the corresponding temporal *stiffness* matrix in the SM-DSEM scheme.

Remark 3.3. The Jacobi polynomials $P_i^{0,\chi}(x)$ in (3.12) and $P_m^{\eta,0}(x)$ in (3.2) have been previously utilized by Li and Xu [23], who formulated exact quadrature rules for the corresponding temporal matrices arising in their Galerkin method. Here, we obtain and interpret the aforementioned polynomials as the asymptotic forms of the polyfractonomial eigenfunctions of FSLPs and employ them in a discontinuous PG framework.

The following lemma is useful in carrying out the temporal fractional integration-by-parts in the development of the SM-DSEM scheme.

LEMMA 3.4 (see [23]). *For all $0 < \xi < 1$, if $u \in H^1([a, b])$, such that $u(a) = 0$, and $w \in H^{\xi/2}([a, b])$, then*

$$({}_a\mathcal{D}_s^\xi u, w)_\Omega = ({}_a\mathcal{D}_s^{\xi/2}u,\ {}_s\mathcal{D}_b^{\xi/2}w)_\Omega, \tag{3.17}$$

where $(\cdot,\cdot)_\Omega$ represents the standard inner product in $\Omega = [a, b]$.

Next, we prove the following lemma that is useful in deriving the weak form in the DSEM-DSEM scheme and discretizing the spatial advection term using the DSEM.

LEMMA 3.5. *For all $0 < \xi < 1$, if $u \in H^1([a, b])$ and $w \in H^{\xi/2}([a, b])$, then*

$$({}_{a^+}\mathcal{D}_s^\xi u, w)_\Omega = ({}_{a^+}\mathcal{D}_s^{\xi/2}u,\ {}_s\mathcal{D}_b^{\xi/2}w)_\Omega. \tag{3.18}$$

Proof. Let $u(a) = u_D \neq 0$ (constant). Then,

$$\begin{aligned}
({}_{a^+}\mathcal{D}_s^{\xi} u, w)_\Omega &= ({}_{a^+}\mathcal{D}_s^{\xi}(u-u_D),\ w)_\Omega + ({}_{a^+}\mathcal{D}_s^{\xi} u_D,\ w)_\Omega, \\
&= ({}_{a^+}\mathcal{D}_s^{\xi/2}(u-u_D),\ {}_{x}\mathcal{D}_s^{\xi/2} w)_\Omega + ({}_{a^+}\mathcal{D}_s^{\xi} u_D,\ w)_\Omega,\ \textit{by Lemma 3.4} \\
&= ({}_{a^+}\mathcal{D}_s^{\xi/2} u, {}_{x}\mathcal{D}_s^{\xi/2} w)_\Omega - ({}_{a^+}\mathcal{D}_s^{\xi/2} u_D, {}_{x}\mathcal{D}_s^{\xi/2} w)_\Omega + ({}_{a^+}\mathcal{D}_s^{\xi} u_D, w)_\Omega.
\end{aligned}$$

Now, it remains to show that $({}_{a^+}\mathcal{D}_s^{\xi} u_D, w)_\Omega = ({}_{a^+}\mathcal{D}_s^{\xi/2} u_D, {}_{x}\mathcal{D}_s^{\xi/2} w)_\Omega$. We note that the lower-terminal of the fractional derivative now is a^+ and not a. Therefore, it does not contradict the previous lemma. Moreover, we can always represent u_D in terms of $Q_n(s) \in C_0^\infty([a,b])$ such that $\forall s \in (a,b), \lim_{N\to\infty} \sum_{n=1}^{N} c_n Q_n(s)$ converges to u_D in a pointwise fashion. Hence,

$$\begin{aligned}
({}_{a^+}\mathcal{D}_s^{\xi} u_D, w)_\Omega &= \left({}_{a^+}\mathcal{D}_s^{\xi} \lim_{N\to\infty} \sum_{n=1}^{N} c_n Q_n(s), w \right)_\Omega \\
&= \left(\lim_{N\to\infty} \sum_{n=1}^{N} c_n [{}_{a^+}\mathcal{D}_s^{\xi/2} Q_n(s)], {}_{s}\mathcal{D}_b^{\xi/2} w \right)_\Omega \\
&\qquad \textit{by Lemma 3.4 since } Q_n(s) \in C_0^\infty([a,b]) \\
&= ({}_{a^+}\mathcal{D}_s^{\xi/2} u_D, {}_{s}\mathcal{D}_b^{\xi/2} w)_\Omega. \qquad \square
\end{aligned}$$

3.3. Implementation of SM-DSEM scheme. Now, we implement the SM-DSEM scheme to solve TSFAE (2.1), where we seek the solution in $\Omega_e = [x_{e-1/2}, x_{e+1/2}] \times [0,T]$ in terms of the linear combination of elements in the basis function space V^e of the form

$$u_{MN}^e(x,t) = \sum_{m=0}^{M} \sum_{n=1}^{N} \hat{u}_{MN}^e \tilde{P}_m^{\eta,0}(x^e)\ {}^{(1)}\tilde{\mathcal{P}}_n^{\mu}(t). \tag{3.19}$$

The ultimate step of the SM-DSEM scheme is to obtain a linear system corresponding to (2.1) of the form

$$\mathsf{A}\ \hat{\mathbf{U}}^e \mathsf{B} + \mathsf{C}\, \hat{\mathbf{U}}^e \mathsf{D} = \mathsf{E} \tag{3.20}$$

for some matrices A, B, C, D, and E, where $\hat{\mathbf{U}}^e$ is the matrix of unknown coefficient in Ω_e and $(\hat{\mathbf{U}}^e)_{mn} = \hat{u}_{mn}^e$. The linear system (3.20) is called the *Lyapunov* matrix equation for which there are several numerical approaches introduced (see, e.g., [15, 29, 34, 38] and references therein). To this end, we require the solution (3.19) to satisfy the following variational (weak) form as

$$\begin{aligned}
\left({}_0\mathcal{D}_t^{\tau/2} u_{MN}^e(x,t),\ {}_t\mathcal{D}_T^{\tau/2} v^e(x,t) \right)_{\Omega_e} &+ \theta \left({}_{x_{e-1/2}^+}\mathcal{D}_x^{\nu/2} u_{MN}^e(x,t),\ {}_{x}\mathcal{D}_{x_{e+1/2}^-}^{\nu/2} v^e(x,t) \right)_{\Omega_e} \\
&+ \gamma_e \left([\![u_{MN}^e(x_{e-1/2},t)]\!],\ v^e(x_{e+1/2}^-,t) \right)_{[0,T]} \\
&= \left(f(x,t), v^e(x,t) \right)_{\Omega_e} - \theta \cdot \mathcal{H}_e^x
\end{aligned} \tag{3.21}$$

$\forall v^e(x,t) \in \mathcal{V}^e$, beginning from the first space-time element, i.e., $e = 1$, and marching element-by-element along the x-axis to $e = N_{el}$. In (3.21), $\gamma_e = -\frac{\theta(\Delta x)_e^{1-\nu}}{(1-\nu)\Gamma(1-\nu)}$,

ALOGRITHM 1. First PG-DG method: A pseudocode for the SM-DSEM scheme, employed in a nonuniformly partitioned domain.

```
Construct S_t and M_t ;
for e = 1; e = N_el do
    Construct M_x^e, S_x^e, and η^e ;
    if e = 1 then
        H_e^x = 0 ;
    else
        Compute H_e^x then construct F^e ;
    end
    Solve M_x^e Û^e S_t^T + (θ S_x^e + γ_e η^e) Û^e M_t^T = F^e ;
end
```

$[\![u^e_{MN}(x_{e-1/2},t)]\!]$ represents the jump discontinuity of the solution at $x = x_{e-1/2}$ as a function of time $t \in [0,T]$, and $(\Delta x)_e = x_{e+1/2} - x_{e-1/2}$ is the (spatial) length of the eth subdomain; also $(\cdot,\cdot)_{\Omega_e}$ and $(\cdot,\cdot)_{[0,T]}$ represent, respectively, the standard inner product in the space-time element Ω_e, i.e.,

$$\Big(f(x,t),g(x,t)\Big)_{\Omega_e} = \int_0^T \int_{x^+_{e-1/2}}^{x^-_{e+1/2}} f(x,t)g(x,t)\; dx\; dt,$$

and the standard inner product in the time interval $[0,T]$ is defined as

$$\Big(p(t),q(t)\Big)_{[0,T]} = \int_0^T p(t)\, q(t)\; dt.$$

Finally, $\mathcal{H}^x_e$ is the *history-load* term, which we shall obtain in a convenient and computationally efficient form shortly.

We obtain the corresponding linear system by plugging the expansion (3.19) into the weak form (3.21), taking $v^e(x,t) = \widetilde{P}_i^{\,0,\chi}(\,x^e\,)\;{}^{(2)}\widetilde{\mathcal{P}}_j^{\,\mu}(\,t\,)$, and choosing $\eta = \chi = \nu/2$ and $\mu = \tau/2$ as the following Lyapunov matrix equation:

$$M^e_x \hat{\mathbf{U}}^e S_t^T \;+\; (\theta S^e_x + \gamma_e \eta^e)\, \hat{\mathbf{U}}^e M_t^T = \mathcal{F}^e, \tag{3.22}$$

where η^e is a constant matrix associated with the eth element and $\hat{\mathbf{U}}^e$ is the unknown $(M+1)\times N$ matirx of coefficients. Moreover, the matrices S_t and M_t represent the corresponding temporal stiffness and mass matrices, and S^e_x and M^e_x denote the spatial stiffness and mass matrices, associated with element Ω_e, respectively. Finally, in (3.22), $\mathcal{F}^e$ is the total load matrix and the superscript ^{T} is the transpose operation.

In Algorithm 1, we present the necessary steps in the SM-DSEM scheme, where the computational domain is assumed to be nonuniformly partitioned. However, dealing with uniform elements, the matrices S_t, M_t, M^e_x, and S^e_x are constructed *once* at a preprocessing step. In the following, we obtain the aforementioned matrices *efficiently* and *exactly*.

Temporal stiffness matrix. S_t is an $N \times N$ *diagonal* matrix whose entries are obtained using (3.8) and (3.16) as

$$(S_t)_{jn} = \int_0^T {}_tD_T^{\tau/2}\ {}^{(2)}\tilde{\mathcal{P}}_j^{\tau/2}(t)\,{}_0D_t^{\tau/2}\ {}^{(1)}\tilde{\mathcal{P}}_n^{\tau/2}(t)dt = \delta_{jn}\left(\frac{2}{T}\right)^{\tau-1}\left(\frac{\Gamma(n+\tau/2)}{\Gamma(n)}\right)^2\frac{2}{2n-1}, \tag{3.23}$$

in which δ_{jn} is the Kronecker delta.

Temporal mass matrix. M_t is also an $N \times N$ matrix whose entries are obtained as

$$(M_t)_{jn} = \int_0^T {}^{(2)}\tilde{\mathcal{P}}_j^{\tau/2}(t)\,{}^{(1)}\tilde{\mathcal{P}}_n^{\tau/2}(t)\ dt, \tag{3.24}$$

which can be computed exactly by mapping $[0, T]$ to the reference element $[-1, 1]$ and employing the Gauss–Lobatto–Jacobi (GLJ) quadrature rule as follows:

$$\begin{aligned}(M_t)_{jn} &= J_t \cdot \int_{-1}^{1} {}^{(2)}\tilde{\mathcal{P}}_j^{\tau/2}(t(s))\,{}^{(1)}\tilde{\mathcal{P}}_n^{\tau/2}(t(s))\ ds \\ &= J_t \cdot \int_{-1}^{1} (1-s)^{\tau/2}\,(1+s)^{\tau/2}\,P_{j-1}^{\tau/2,-\tau/2}(s)P_{n-1}^{-\tau/2,\tau/2}(s)ds \\ &= J_t \cdot \sum_{k=0}^{Q-1} w_k^{\tau/2,\tau/2}\ P_{k-1}^{\tau/2,-\tau/2}(s_k)\,P_{n-1}^{-\tau/2,\tau/2}(s_k),\end{aligned} \tag{3.25}$$

when $2Q - 3 = 2(N - 1)$. In (3.25), $J_t = (T/2)$ represents the Jacobian of the transformation, and $\{s_k\}_{k=0}^{Q-1}$ and $\{w_k^{\tau/2,\tau/2}\}_{k=0}^{Q-1}$ are the corresponding quadrature points and weights, associated with GLJ rule.

Spatial stiffness matrix. S_x^e is an $(M + 1) \times (M + 1)$ matrix whose entries are obtained as

$$(S_x^e)_{im} = \int_{x_{e-1/2}}^{x_{e+1/2}} {}_{x_{e-1/2}}\mathcal{D}_x^{\nu/2}\tilde{P}_i^{\nu/2,0}(x)\,{}_x\mathcal{D}_{x_{e+1/2}}^{\nu/2}\tilde{P}_m^{0,\nu/2}(x)dx, \tag{3.26}$$

which can be computed exactly by mapping $[x_{e-1/2}, x_{e+1/2}]$ to the reference element $[-1, 1]$ and employing another GLJ rule corresponding to a different weight function as follows:

$$\begin{aligned}(S_x^e)_{im} &= C_x^e \cdot \int_{-1}^{1} {}_{-1}\mathcal{D}_z^{\nu/2}\tilde{P}_i^{\nu/2,0}(x(z))\,{}_z\mathcal{D}_1^{\nu/2}\tilde{P}_m^{0,\nu/2}(x(z))dz \\ &= C_x^e \cdot \Lambda_{im}\int_{-1}^{1}(1-z)^{-\nu/2}\,(1+z)^{-\nu/2}\ P_i^{\nu,-\nu/2}(z)\,P_m^{-\nu/2,\nu}(z) \\ &= C_x^e \cdot \Lambda_{im}\ \sum_{k=0}^{M} P_i^{\nu,-\nu/2}(z_k)P_m^{-\nu/2,\nu}(z_k)\rho_k^{-\nu/2,-\nu/2},\end{aligned} \tag{3.27}$$

where $C_x^e = (2/\Delta x_e)^{\nu-1}$, and

$$\Lambda_{im} = \frac{\Gamma(i+1)}{\Gamma(i-\nu/2+1)}\frac{\Gamma(m+1)}{\Gamma(m-\nu/2+1)}.$$

Moreover, $\{z_k\}_{k=0}^{M}$ and $\{\rho_k\}_{k=0}^{M}$ are the corresponding GLJ quadrature points and weights in the interval $[-1,1]$, associated with the weight function $(1-z)^{-\nu/2}(1+z)^{-\nu/2}$. Here, we have used the relations (3.7) and (3.15) to obtain

$$
\begin{aligned}
{}_{-1}\mathcal{D}_z^{\nu/2} P_m^{\nu/2,0}(z) &= \frac{\Gamma(m+1)}{\Gamma(m-\tau/2+1)}(1+z)^{-\nu/2} P_m^{\nu,-\nu/2}(z),\\
{}_{z}\mathcal{D}_1^{\nu/2} P_i^{0,\nu/2}(z) &= \frac{\Gamma(i+1)}{\Gamma(i-\tau/2+1)}(1-z)^{-\nu/2} P_i^{-\nu/2,\nu}(z)
\end{aligned}
$$

in the reference element, employed in (3.27).

Spatial mass matrix. M_x^e is also an $(M+1)\times(M+1)$ matrix whose entries are defined as

$$
(M_x^e)_{im} = \int_{x_{e-1/2}}^{x_{e+1/2}} \tilde{P}_i^{0,\nu/2}(x_e)\tilde{P}_m^{\nu/2,0}(x_e)dx, \tag{3.28}
$$

where we compute the mass matrix exactly and use the standard Gauss–Lobato–Legendre (GLL) rule by choosing Q so that $2Q-3=2M$

$$
\begin{aligned}
(M_x^e)_{im} &= J_x^e \int_{-1}^{1} P_i^{0,\nu/2}(x(\xi))P_m^{\nu/2,0}(x(\xi))d\xi \\
&= J_x^e \sum_{k=0}^{Q} w_k P_i^{0,\nu/2}(\xi_k)P_m^{\nu/2,0}(\xi_k),
\end{aligned} \tag{3.29}
$$

where $J_x^e = (\Delta x_e)/2 = 1/2(x_{e+1/2}-x_{e-1/2})$ is the Jacobian of the transformation.

Constant matrix. η^e is also an $(M+1)\times(M+1)$ matrix whose entries are defined as

$$
\begin{aligned}
(\eta^e)_{im} &= P_i^{0,\nu/2}(+1)\, P_m^{\nu/2,0}(-1)\\
&= P_m^{\nu/2,0}(-1)\\
&= (-1)^m
\end{aligned} \tag{3.30}
$$

for $m=0,1,2,\ldots,M$.

Total load matrix. $\mathcal{F}^e$ is an $(M+1)\times(N)$ matrix defined in terms of the aforementioned stiffness and mass matrices

$$
\mathcal{F}^e = F^e - \gamma_e \eta^e \hat{\mathbf{U}}^{e-1} M_t^T - \theta\, \mathcal{H}_e^x \tag{3.31}
$$

in which $F^e = (f(x,t), v^e(x,t))_{\Omega_e}$, $\hat{\mathbf{U}}^{e-1}$ denotes the coefficient matrix, known in the previously resolved element I_{e-1}, and we obtain the history-load term $\mathcal{H}_e^x$ in a computationally efficient form as

$$
(\mathcal{H}_e^x)_{ij} = F_e(x)P_i^{0,\nu/2}(x)\big|_{x=x_{e-1/2}^{+}}^{x=x_{e+1/2}^{-}} - \int_{x_{e-1/2}}^{x_{e+1/2}} F_e(x)\frac{d}{dx}P_i^{0,\nu/2}(x)\, dx, \tag{3.32}
$$

in which $F_e(x)$ represents the history function associated with the current element Ω_e

$$
F_e(x) = \sum_{\varepsilon=1}^{e-1} F_e^{\varepsilon}(x), \tag{3.33}
$$

consisting of all the past element contributions as

$$F_e^{\varepsilon}(x) = \sum_{m,n} \hat{u}_{mn}^{\varepsilon} \, (M_t)_{jn} \sum_{\delta=0}^{M} \Big(C_\delta \cdot (x-s)^{\delta+1-\nu} \Big) \tilde{P}_m^{\nu/2,0(\delta)}(s) \Big|_{s=s^{-}_{\varepsilon+1/2}}^{s=s^{+}_{\varepsilon-1/2}}, \tag{3.34}$$

where $\tilde{P}_m^{\nu/2,0(\delta)}(s)$ represents the δth derivative of $\tilde{P}_m^{\nu/2,0}(s)$. The coefficient $C_\delta = -1/\{\Gamma(1-\nu)\prod_{k=0}^{\delta}(k+1-\nu)\}$ decays in a factorial fashion with respect to δ. We note that when $e = 1$, there is no history introduced into the problem, hence $(\mathcal{H}_1^x)_{ij} \equiv 0$.

In Figure 1, we present the h-refinement (left panel) and p-refinement (right panel) tests for SM-DSEM. For the case of h-refinement, we present the log-log L^2-error versus the number of elements N_{el}, corresponding to piecewise linear/cubic spatial bases and $\nu = 1/10$, $9/10$ while $\tau = 1/2$. Associated with the p-refinement, we plot the log-linear L^2-error versus M or N the spatial/temporal order-indices in (3.19). In the spatial p-refinement, the spatial orders $\nu = 1/10$ and $9/10$, while $\tau = 1/2$, also in the temporal p-refinement $\tau = 1/10$ and $9/10$, while $\nu = 1/2$. The first row corresponds to $u^{ext}(x,t) = t^{10}\, x^{13/2} \sin(\pi x^{4/3})$, the second row to $u^{ext}(x,t) = t^6 \sin(\pi t)\, [x^{13/2} \sin(\pi x^{4/3})]$, and the third row to $u(x,t) = t^{10}[x^6 \exp(x^2) + x^{8+5/7} + x^{10+1/3}]$. We observe an exponential-like convergence in p-refinement and the algebraic convergence in h-refinement.

In all the above cases, the exact solutions are relatively smooth. We examine a case where the exact solution does not belong to higher Sobolev spaces. For this case, we confirm the success of h-refinement in Figure 2. In this plot, we present the log-log L^2-error versus number of elements N_{el}, corresponding to piecewise linear/cubic spatial bases, temporal order $N = 13$ fixed, $\tau = \nu = 1/2$, and the exact solution $u^{ext}(x,t) = t^{10}\, x^{1+3/7}$, which is not smooth with respect to x.

4. Time-integration using SM-DSEM when $\tau = 1$. We recall that SM-DSEM works equally well when the temporal time-derivative order τ tends to 1. In general, a PDE/FPDE, which is first-order in time, reads as

$$\frac{\partial u}{\partial t} = F(u; x, t), \tag{4.1}$$

where particularly in view of (2.1), the operator $F(u;x,t)$ is given as

$$F(u;x,t) = f(x,t) - \theta \; {}_0\mathcal{D}_x^{\nu} u(x,t).$$

Here, we regard the PG-DG method as an alternative scheme for *spectrally* accurate time-integration for a general $F(u;x,t)$, rather than utilizing existing *algebraically* accurate methods, including *multistep* methods such as the Adams family and stifflystable schemes and *multistage* approaches such as the Runge–Kutta method.

The idea of employing SM-DSEM when $\tau = 1$ is simply based on the useful property by which a full first-order derivative d/dt can be decomposed into a product of the sequential $(\frac{1}{2})$th-order derivatives ${}_0\mathcal{D}_t^{1/2}\, {}_0\mathcal{D}_t^{1/2}$, a result that is not valid in the standard (integer-order) calculus. Hence, by virtue of the *fractional* integration-by-parts (see Lemma 3.4), such a decomposition artificially induces *nonlocality* to the temporal term in the corresponding weak form. Therefore, it provides an appropriate framework for *global* (spectral) treatment of the temporal term using SM-DSEM.

To demonstrate the efficiency of SM-DSEM when ${}_0\mathcal{D}_t^{\tau} \to d/dt$, we compare the computational cost of SM-DSEM with that of the multistep methods such as SSS,

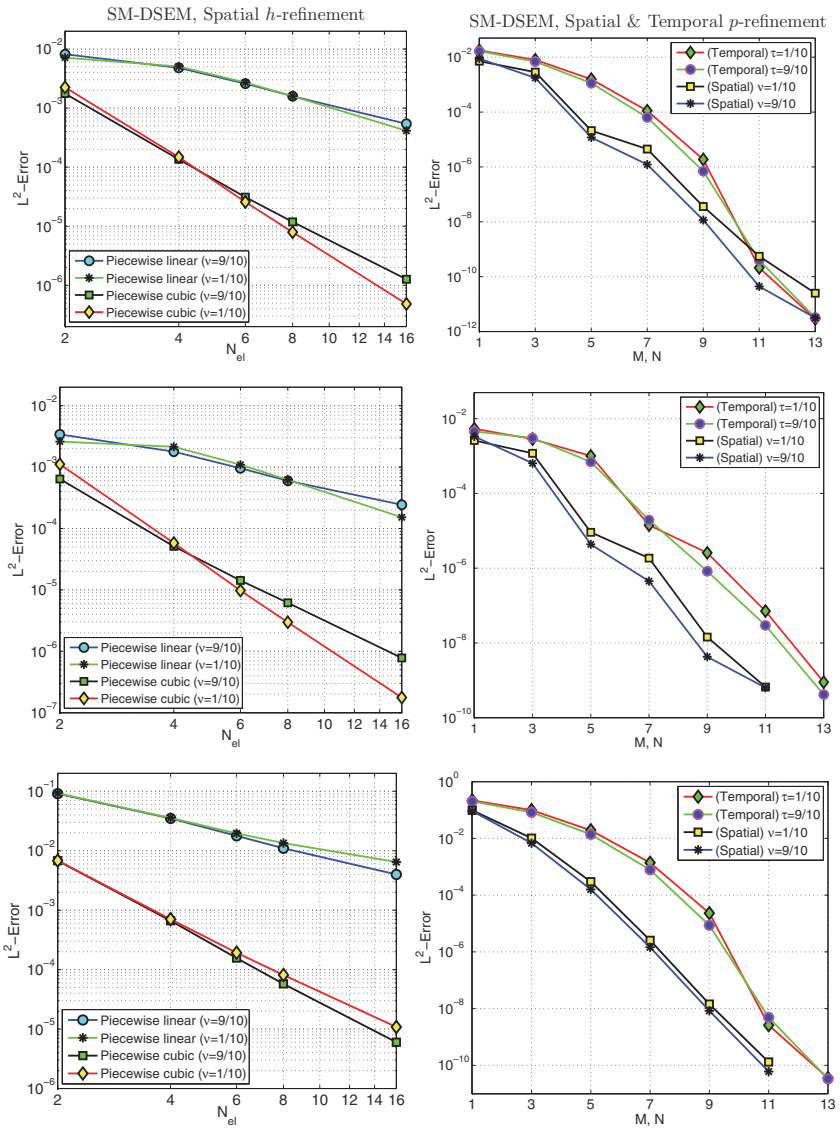

FIG. 1. *SM-DSEM. (Left) h-refinement: log-log L^2-error versus number of elements N_{el}, corresponding to piecewise linear/cubic spatial bases and $\nu = 1/10,\ 9/10$ while $\tau = 1/2$. (Right) p-refinement: log-linear L^2-error versus M/N the spatial/temporal order-indices in* (3.19). *In the spatial p-refinement, the spatial orders are $\nu = 1/10$ and $9/10$ while $\tau = 1/2$, also in the temporal p-refinement $\tau = 1/10$ and $9/10$ while $\nu = 1/2$. The first row corresponds to $u^{ext}(x,t) = t^{10}\, x^{13/2} \sin(\pi x^{4/3})$, the second row to $u^{ext}(x,t) = t^6 \sin(\pi t)\, [x^{13/2} \sin(\pi x^{4/3})]$, and the third row to $u(x,t) = t^{10}[x^6 \exp(x^2) + x^{8+5/7} + x^{10+1/3}]$.*

Adams–Bashforth (AB), and Adams–Moulton (AM). To this end, we recall these schemes to integrate (4.1) in time, where we employ DSEM to discretize the spatial domain as before. However, we note that our approach is independent of the type of the spatial discretization.

In Table 1, we present the CPU time (seconds) corresponding to the backward and forward multistep time-integration schemes introduced along with that of our

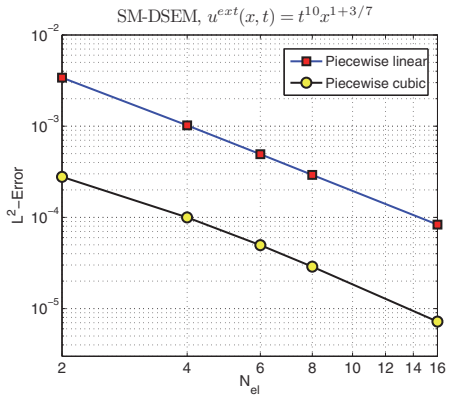

FIG. 2. *SM-DSEM. h-refinement: log-log L^2-error versus number of elements N_{el}, corresponding to piecewise linear/cubic spatial bases, temporal order $N = 13$ fixed, $\tau = \nu = 1/2$, and the exact solution $u^{ext}(x,t) = t^{10}\, x^{1+3/7}$.*

TABLE 1

CPU time (seconds) on a dual-core 2.9 GHz Intel processor, corresponding to the third-order in time SSS-DSEM, AB-DSEM, AM-DSEM, and our high-order SM-DSEM scheme all with two elements in space and polynomial order $M = 3$. The spatial fractional order is $\nu = 1/2$ and the temporal time-order is $\tau = 1$. Here, the simulation time $T = 1$.

L^2-error	SSS-DSEM	AB-DSEM	AM-DSEM	SM-DSEM
$\mathcal{O}(10^{-4})$	8.5830	15.9770	9.2260	($N = 7$) 11.2020
$\mathcal{O}(10^{-8})$	117.423	328.655	136.976	($N = 13$) 28.634
$\mathcal{O}(10^{-9})$	233.153	652.611	272.125	($N = 15$) 37.619
$\mathcal{O}(10^{-10})$	463.874	1302.793	685.618	($N = 17$) 48.919

SM-DSEM. We particularly compare the CPU time in the third-order SSS-DSEM, AB-DSEM, AM-DSEM, and our SM-DSEM developed in section 3.3. We choose the exact solution to be $u^{ext}(x,t) = x^3 t^{13/2} \sin(\pi t^{4/3})$, where we consider two elements in space and setting the polynomial order $M = 3$ to accurately resolve the spatial solution. Moreover, we set the spatial fractional order to $\nu = 1/2$ and set the temporal time-order to the integer value $\tau = 1$. Among the multistep methods, we observe SSS-DSEM to be more efficient than AB-DSEM and AM-DSEM, especially at smaller error-levels. Moreover, Table 1 shows that all the aforementioned schemes are comparable in terms of the CPU time at the relatively large L^2-error $\mathcal{O}(10^{-4})$. However, SM-DSEM outperforms all the multistep methods by about one order of magnitude speed-up at smaller error levels.

5. DG-DG method: DSEM-in-time and DSEM-in-space. We extend our SM-DSEM scheme to another method, which is more appropriate for adaptive and/or long-time integration of (2.1). The idea is to discretize both the space- and time-domain employing DSEM in an *hp*-element fashion. We set $\tau \in (0,1)$ and $\nu \in (0,1)$ in (2.1), subject to homogeneous Dirichlet initial/boundary conditions. In DSEM-DSEM, we first decompose the space-domain $[0, L]$ into N_{el}^x nonoverlapping subintervals $I_{\widetilde{e}}^x = [x_{\widetilde{e}-1/2}, x_{\widetilde{e}+1/2}]$ and the time-domain $[0, T]$ into N_{el}^t subintervals $I_{\widehat{e}}^t = [t_{\widehat{e}-1/2}, t_{\widehat{e}+1/2}]$. Next, we partition the whole computational domain $\Omega = [0, L] \times [0, T]$ into $\mathcal{N}^{el} = N_{el}^x \cdot N_{el}^t$ *structured* space-time elements $\Omega_e \equiv I_{\widetilde{e}}^x \times I_{\widehat{e}}^t$ such that $\cup_{e=1}^{\mathcal{N}^{el}} \Omega_e = \Omega$. In this setting, the element number e corresponds to a particular pair of the spatial subinterval number $\widetilde{e}$ and the temporal one $\widehat{e}$, respectively.

5.1. Basis and test function spaces in DSEM-DSEM scheme. We construct the basis function space $\mathbf{V}^e$ as the tensor product of the asymptotic (temporal and spatial) eigenfunctions, presented in section 3.3, as

$$\mathbf{V}^e \equiv span\{\widetilde{P}_m^{\eta^x,0}(x_{\widetilde{e}})\,\widetilde{P}_n^{\eta^t,0}(t_{\widehat{e}}) : m = 0,1,\dots,M, n = 0,1,\dots,N\}, \tag{5.1}$$

where $\eta^x,\ \eta^t \in (0,1)$ and the temporal bases $\widetilde{P}_n^{\eta^t,0}(\,t_{\widehat{e}}\,)$ are Jacobi polynomials, defined in the time-interval $I_{\widehat{e}}^t = [t_{\widehat{e}-1/2},\, t_{\widehat{e}+1/2}]$ as the asymptotic eigenfunction $P_n^{\eta^t,0}(\,\xi\,)$ through an affine mapping from the standard domain $[-1,1]$ to the physical time-subdomain $I_{\widehat{e}}^t$. We approximate the solution to (2.1) in Ω_e in terms of linear combination of elements in $\mathbf{V}^e$. In our PG DSEM-DSEM scheme, we construct the space of test functions $\mathbb{V}^e$, constructed as

$$\mathbb{V}^e \equiv span\{\widetilde{P}_i^{0,\chi^x}(x_{\widetilde{e}})\,\widetilde{P}_j^{0,\chi^t}(t_{\widehat{e}}) : i = 0,1,\dots,M, j = 0,1,\dots,N\}, \tag{5.2}$$

where we test problem (2.1) against elements in $\mathbb{V}^e$.

5.2. Implementation of DSEM-DSEM scheme. The space-time basis functions in our DSEM-DSME are *discontinuous* in both space and time at the interfaces of the two-dimensional (time-space) element Ω_e. Here, we seek the approximation solution to (2.1), restricted in element Ω_e, of the form

$$u(x,t)\big|_{\Omega_e} \approx u_{MN}^e(x,t) = \sum_{m=0}^{M}\sum_{n=0}^{N} \overline{u}_{mn}^{\,e}\widetilde{P}_m^{\eta^x,0}(\,x_{\widetilde{e}}\,),\widetilde{P}_n^{\eta^t,0}(\,t_{\widehat{e}}\,). \tag{5.3}$$

Once again the ultimate step in our DSEM-DSEM scheme is to construct a linear system corresponding to (2) of Lyapunov form (3.20). To this end, we require the solution (5.3) to satisfy the following weak form:

$$\begin{aligned}
&\Big({}_{t^+_{\widehat{e}-1/2}}\mathcal{D}_t^{\tau/2}u_{MN}^e(x,t)\,,\,{}_t\mathcal{D}^{\tau/2}_{t^-_{\widehat{e}+1/2}}v^e(x,t)\Big)_{\Omega_e}\\
&\quad+\theta\Big({}_{x^+_{\widetilde{e}-1/2}}\mathcal{D}_x^{\nu/2}u_{MN}^e(x,t),\,{}_x\mathcal{D}^{\nu/2}_{x^-_{\widetilde{e}+1/2}}v^e(x,t)\Big)_{\Omega_e}\\
&\quad+\gamma_{\widetilde{e}}^{\,x}\Big(\llbracket u_{MN}^e(x_{\widetilde{e}-1/2},\,t)\rrbracket,\ v^e(x^-_{\widetilde{e}+1/2},\,t)\Big)_{I_{\widehat{e}}^t}\\
&\quad+\gamma_{\widehat{e}}^{\,t}\Big(\llbracket u_{MN}^e(x,\,t_{\widehat{e}-1/2})\rrbracket,\ v^e(x,\,t^-_{\widehat{e}+1/2})\Big)_{I_{\widetilde{e}}^x}\\
&\quad=\Big(f(x,t),v^e(x,t)\Big)_{\Omega_e}-\theta\cdot\mathcal{H}_{\widetilde{e}}^x-\mathcal{H}_{\widehat{e}}^t
\end{aligned} \tag{5.4}$$

$\forall v^e(x,t)\in\mathbb{V}^e$. In (5.4),

$$\gamma_{\widetilde{e}}^{\,x} = -\frac{\theta(\Delta x)_{\widetilde{e}}^{1-\nu}}{(1-\nu)\Gamma(1-\nu)} \tag{5.5}$$

and

$$\gamma_{\widehat{e}}^{\,t} = -\frac{(\Delta t)_{\widehat{e}}^{1-\tau}}{(1-\tau)\Gamma(1-\tau)}, \tag{5.6}$$

where $(\Delta x)_{\widetilde{e}} = x_{\widetilde{e}+1/2} - x_{\widetilde{e}-1/2}$ and $(\Delta t)_{\widehat{e}} = t_{\widehat{e}+1/2} - t_{\widehat{e}-1/2}$. Moreover, $\llbracket u_{MN}^e(x_{\widetilde{e}-1/2},\,t)\rrbracket$ denotes the (spatial) jump discontinuity of the solution at

$x = x_{\widetilde{e}-1/2}$ as a function of time $t \in I_{\widehat{e}}^t$ and $[\![u_{MN}^e(x, t_{\widehat{e}-1/2})]\!]$ is the (temporal) jump discontinuity of the solution at $t = t_{\widehat{e}-1/2}$ as a function of space $x \in I_{\widetilde{e}}^x$. Similarly, $(\cdot,\cdot)_{\Omega_e}$, $(\cdot,\cdot)_{I_{\widehat{e}}^t}$, and $(\cdot,\cdot)_{I_{\widetilde{e}}^x}$ are, respectively, the standard inner product in the local space-time element Ω_e

$$\Big(f(x,t), g(x,t)\Big)_{\Omega_e} = \int_{I_{\widehat{e}}^t}\int_{I_{\widetilde{e}}^x} f(x,t)g(x,t)\; dx\; dt,$$

the inner product in $I_{\widehat{e}}^t$, defined as

$$\Big(p(t), q(t)\Big)_{I_{\widehat{e}}^t} = \int_{t_{\widehat{e}-1/2}^+}^{t_{\widehat{e}+1/2}^-} p(t)\, q(t)\; dt,$$

and the inner product in $I_{\widetilde{e}}^x$

$$\Big(Y(x), W(x)\Big)_{I_{\widetilde{e}}^x} = \int_{x_{\widetilde{e}-1/2}^+}^{x_{\widetilde{e}+1/2}^-} Y(x)\, W(x)\; dx.$$

Finally, in (5.4), $\mathcal{H}_{\widetilde{e}}^x$ and $\mathcal{H}_{\widehat{e}}^t$ represent the corresponding *spatial history-load* and *temporal history-load* term, which we compute in an efficient fashion similar to that presented in section 3.3.

Next, we obtain the corresponding linear system resulting from our DSEM-DSEM scheme by substituting the solution (5.3) into the weak form (5.4), taking $v^e(x,t) = \widetilde{P}_i^{\,0,\chi^x}(\,x_{\widetilde{e}}\,)\,\widetilde{P}_j^{\,0,\chi^t}(\,t_{\widehat{e}}\,)$, and choosing $\eta^x = \chi^x = \nu/2$ and $\mu = \tau/2$ as another *Lyapunov* equation,

$$M_x^{\widetilde{e}}\;\overline{\mathbf{U}}^{\,e}\;\left(S_t^{\widehat{e}\;T} + \gamma_{\widehat{e}}^{\,t}\eta^{\widehat{e}}\right) + \left(\theta S_x^{\widetilde{e}} + \gamma_{\widetilde{e}}^{\,x}\eta^{\widetilde{e}}\right)\;\overline{\mathbf{U}}^{\,e}\;\; M_t^{\widehat{e}\;T} = \mathbb{F}^e, \tag{5.7}$$

where we recall that the element number e is associated with the pair of $\widetilde{e}$ and $\widehat{e}$, the spatial and temporal subintervals $I_{\widetilde{e}}^x$ and $I_{\widehat{e}}^t$. In the Lyapunov system (5.7), $\overline{\mathbf{U}}^{\,e}$ is the $(M+1)\times(N+1)$ matrix of unknown coefficient associated with Ω_e whose entries are $\overline{\mathbf{U}}_{mn}^{\,e} = \overline{u}_{mn}^{\,e}$. In addition, the spatial matrices $S_x^{\widetilde{e}}$, $M_x^{\widetilde{e}}$, and $\eta^{\widetilde{e}}$ represent the corresponding $(M+1)\times(M+1)$ spatial stiffness, mass, and constant matrices, respectively, which are identical to those obtained in (3.27), (3.29), and (3.30), by setting e to $\widetilde{e}$. Moreover, $S_t^{\widehat{e}}$, $M_t^{\widehat{e}}$, and $\eta^{\widehat{e}}$ are, respectively, the temporal stiffness, mass, and constant matrices.

In Algorithm 2, we present the corresponding pseudocode for our DSEM-DSEM scheme, where the computational space- and time-domain are assumed to be non-uniformly partitioned. As before, if the elements are uniform, we construct the matrices $M_x^{\widetilde{e}}$, $S_x^{\widetilde{e}}$, $\eta^{\widetilde{e}}$, also $M_t^{\widehat{e}}$, $S_t^{\widehat{e}}$, and $\eta^{\widehat{e}}$, only *once* at a preprocessing step. In the following, we present the construction of the corresponding temporal matrices.

Temporal stiffness matrix. $S_t^{\widehat{e}}$ is an $(N+1)\times(N+1)$ matrix whose entries are obtained as

$$\begin{aligned}(S_t^{\widehat{e}})_{jn} &= \int_{t_{\widehat{e}-1/2}}^{t_{\widehat{e}+1/2}} {}_{t_{\widehat{e}-1/2}}\mathcal{D}_t^{\tau/2}\tilde{P}_j^{\tau/2,0}(t_{\widehat{e}})\;{}_t\mathcal{D}_{t_{\widehat{e}+1/2}}^{\tau/2}\tilde{P}_n^{0,\tau/2}(t_{\widehat{e}})dt \\ &= C_t^{\widehat{e}}\cdot\Lambda_{im}^t\sum_{k=0}^{N} P_j^{\tau,-\tau/2}(z_k)P_n^{-\tau/2,\tau}(z_k)\rho_k^{-\tau/2,-\tau/2},\end{aligned} \tag{5.8}$$

ALOGRITHM 2. Pseudocode of DSEM-DSEM scheme, employed in a nonuniform structured partitioned domain.

for $e = 1$; $e = N_{el}$ **do**
  Construct $M_x^{\widetilde{e}}$, $S_x^{\widetilde{e}}$, $\eta^{\widetilde{e}}$, also $M_t{}^{\widehat{e}}$, $S_t{}^{\widehat{e}}$, and $\eta^{\widehat{e}}$;
  if $e = 1$ **then**
    $\mathcal{H}_{\widetilde{e}}^x = 0$ and $\mathcal{H}_{\widehat{e}}^t = 0$;
  else
    Compute $\mathcal{H}_{\widetilde{e}}^x$ and $\mathcal{H}_{\widehat{e}}^t$ then construct $\mathbb{F}^e$;
  end
  Solve $M_x^{\widetilde{e}}\ \overline{\mathbf{U}}^e\ (S_t^{\widehat{e}\ T} + \gamma_{\widehat{e}}{}^t \eta^{\widehat{e}})\ +\ (\theta S_x^{\widetilde{e}} + \gamma_{\widetilde{e}}{}^x \eta^{\widetilde{e}})\ \overline{\mathbf{U}}^e\ M_t^{\widehat{e}\ T} = \mathbb{F}^e$;
end

which we compute *exactly* by mapping $[t_{\widehat{e}-1/2}, t_{\widehat{e}+1/2}]$ to the reference element $[-1, 1]$ and performing a GLJ rule similar to (3.27). Here, $C_t^{\widehat{e}} = \{2/(\Delta t)_{\widehat{e}}\}^{\tau-1}$, and

$$\Lambda_{jn}^t = \frac{\Gamma(j+1)}{\Gamma(j-\tau/2+1)} \frac{\Gamma(n+1)}{\Gamma(n-\tau/2+1)}.$$

Moreover, $\{z_k\}_{k=0}^N$ and $\{\rho_k\}_{k=0}^N$ are the corresponding GLJ quadrature points and weights in the interval $[-1, 1]$, associated with the weight function $(1-z)^{-\tau/2}(1+z)^{-\tau/2}$.

Temporal mass matrix. $M_t{}^{\widehat{e}}$ is also an $(N+1) \times (N+1)$ matrix whose entries are obtained as

$$\begin{aligned}(M_t{}^{\widehat{e}})_{jn} &= \int_{t_{\widehat{e}-1/2}}^{t_{\widehat{e}+1/2}} \tilde{P}_j^{0,\tau/2}(t_{\widehat{e}}) \tilde{P}_n^{\tau/2,0}(t_{\widehat{e}}) dx \\ &= J_t^{\widehat{e}} \sum_{k=0}^{Q} w_k P_j^{0,\tau/2}(\xi_k) P_m^{\tau/2,0}(\xi_k),\end{aligned} \tag{5.9}$$

in which $J_t^{\widehat{e}} = (\Delta x)_{\widehat{e}}/2$ is the Jacobian of the transformation from the time subinterval to the standard element. Here, we compute the mass matrix *exactly* based on the standard GLL rule and choosing Q so that $2Q - 3 = 2N$ similar to (3.25).

Constant matrix. $\eta^{\widehat{e}}$ is also an $(M+1) \times (M+1)$ matrix whose entries are defined as

$$\begin{aligned}(\eta^e)_{jn} &= P_j^{0,\tau/2}(+1)\, P_n^{\tau/2,0}(-1) \\ &= (-1)^n\end{aligned} \tag{5.10}$$

for $j, n = 0, 1, 2, \ldots, N$.

Total load matrix. $\mathbb{F}^e$ is an $(M+1) \times (N+1)$ matrix defined as

$$\mathbb{F}^e = \mathbf{F}^e - \gamma_{\widetilde{e}}{}^x \left(\eta^{\widetilde{e}}\ \hat{\mathbf{U}}^{e-1} M_t^{\widehat{e}\ T}\right) - \gamma_{\widehat{e}}{}^t \left(M_x^{\widetilde{e}\ T}\ \hat{\mathbf{U}}^{e-1}\ \eta^{\widehat{e}}\right) - \theta\, \mathcal{H}_{\widetilde{e}}^x - \mathcal{H}_{\widehat{e}}^t \tag{5.11}$$

in which $\mathbf{F}^e = (f(x,t), v^e(x,t))_{\Omega_e}$, and $\hat{\mathbf{U}}^{e-1}$ denotes the coefficient matrix, known in the previously resolved element Ω_{e-1}, and we obtain the spatial and temporal history-load terms $\mathcal{H}_{\widetilde{e}}^x$ and $\mathcal{H}_{\widehat{e}}^t$ in a similar computationally efficient form as

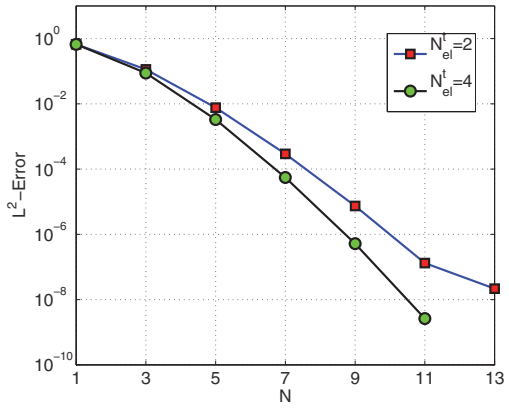

FIG. 3. *DSEM-DSEM. Long-time integration: log-linear L^2-error versus the temporal order-index N in (5.3), corresponding to $N^t_{el} = 2$ and 4 temporal subintervals, and $N^x_{el} = 2$ spatial subintervals kept fixed, i.e., total $N_{el} = N^x_{el}.N^t_{el} = 4$ and 8 space-time elements. Here, the simulation time $T = 10$ and $\tau = \nu = 1/2$.*

$$(\mathcal{H}^x_{\widetilde{e}})_{ij} = F_e(x)P_i^{0,\nu/2}(x)\Big|_{x=x^-_{\widetilde{e}+1/2}}^{x=x^+_{\widetilde{e}-1/2}} - \int_{x_{\widetilde{e}-1/2}}^{x_{\widetilde{e}+1/2}} F_e(x)\frac{d}{dx}P_i^{0,\nu/2}(x)\,dx \tag{5.12}$$

and

$$(\mathcal{H}^t_{\widetilde{e}})_{ij} = G_e(t)P_j^{0,\tau/2}(t)\Big|_{t=t^-_{\widehat{e}+1/2}}^{t=t^+_{\widehat{e}-1/2}} - \int_{t_{\widehat{e}-1/2}}^{t_{\widehat{e}+1/2}} G_e(t)\frac{d}{dt}P_j^{0,\tau/2}(t)\,dt, \tag{5.13}$$

respectively. We then obtain the corresponding spatial history functions $F_e(x)$ in (3.33), setting e to $\widetilde{e}$. Similarly, we obtain the temporal history function $G_e(x)$ associated with the current element Ω_e as

$$G_e(t) = \sum_{\varepsilon=1}^{\widehat{e}-1} G^{\varepsilon}_{\widehat{e}}(t), \tag{5.14}$$

in which

$$G^{\varepsilon}_{\widehat{e}}(t) = \sum_{m,n}\hat{u}^{\varepsilon}_{mn}\,(M^{\widetilde{e}}_x)_{im}\sum_{\delta=0}^{N}\Big(C^t_\delta\cdot(t-s)^{\delta+1-\tau}\Big)\tilde{P}_n^{\,\tau/2,0(\delta)}(s)\Big|_{s=s^+_{\varepsilon-1/2}}^{s=s^-_{\varepsilon+1/2}}, \tag{5.15}$$

where the coefficient $C^t_\delta = -1/\{\Gamma(1-\tau)\prod_{k=0}^{\delta}(k+1-\tau)\}$.

We have examined the DSEM-DSEM for all the test-cases presented previously successfully. Here, we examine DSEM-DSEM for log-time integration. In Figure 3, and corresponding to the simulation time $T = 10$ and $\tau = \nu = 1/2$, we plot the log-linear L^2-error versus the temporal order-index N in (5.3). We partition the whole computational domain into 4 and 8 elements by choosing $N^t_{el} = 2$ and 4 and choosing $N^x_{el} = 2$ fixed. While we have increased the simulation time from $T = 1$ to $T = 10$, we recover the spectral convergence in DSEM-DSEM.

6. Summary and discussion. We have developed high-order methods for TSFAE of the form (2.1), subject to Dirichlet initial/boundary conditions. We have presented two highly accurate. We first developed the SM-DSEM scheme for carrying out the time-integration using a single time-domain SM and performing the

TABLE 2

Inhomogeneous boundary conditions. p-refinement in the spatial dimension for Case I, $u^{ext}(x,t) = t^{3+1/2}\cos(\pi x)$, *and for Case* II, $u^{ext}(x,t) = t^{10}[exp(x^2)+10\pi]$. *Here, we set* $T = L = 1$, $\tau = \nu = 1/2$, *and* $N = 15$.

M	L^2-error, case I	L^2-error, case II
1	0.0384286	0.334819
3	0.0007635	0.001144
5	4.98×10^{-6}	1.71×10^{-5}
7	6.18×10^{-8}	1.54×10^{-7}

spatial discretization using DSEM, when $\tau \in (0,1]$, $\nu \in (0,1)$. We accomplished this based on the new spectral theory for FSLPs, presented in [40], which provides proper spaces of basis and test functions. For the particular case $\tau = 1$, we presented this PG-DG method as a spectrally accurate time-integration method, which outperforms the existing algebraically accurate backward and forward multistep methods in terms of cost and accuracy. We subsequently extended the SM-DSEM to another method, DSEM-DSEM, in which both time-integration and spatial discretization are performed in an *hp*-element fashion, when $\tau \in (0,1)$, $\nu \in (0,1)$. We presented numerical tests in each case to demonstrate the exponential-like convergence of our methods employing *p*-refinement, in addition to the algebraic convergence in DSEM when *h*-refinement is performed.

Although we have formulated the aforementioned methods when (2.1) is subject to *homogeneous* Dirichlet boundary and initial conditions, i.e., $h(t) = g(x) = 0$, these schemes are equally valid when *inhomogeneous* conditions are enforced. In such cases, we first homogenize the problem by the method of *lifting a known solution*. Using this trick, we first set the solution $u(x,t) = u^H(x,t) + g(x) + h(t)$ and then substitute in (2.1). Hence, we obtain a modified/homogenized TSFAE of the form

$$
\begin{aligned}
{}_0\mathcal{D}_t^{\tau} u^H(x,t) + \theta\ {}_0\mathcal{D}_x^{\nu} u^H(x,t) &= \widetilde{f}(x,t), \quad (x,t) \in [0,L] \times [0,T], \\
u^H(x,0) &= 0, \\
u^H(0,t) &= 0,
\end{aligned}
\tag{6.1}
$$

where $\widetilde{f} = f - ({}_0\mathcal{D}_t^{\tau} + \theta\ {}_0\mathcal{D}_x^{\nu})\{h(t) + g(x)\}$, and we recall that $h(0) = g(0)$. For demonstration of the generality of the schemes presented, we solve (2.1) subject to inhomogeneous boundary conditions, e.g., using SM-DSEM. We consider the following two test-cases: (i) the exact solution $u^{ext}(x,t) = t^{3+1/2}\cos(\pi x)$, corresponding to the time-variable inhomogeneous boundary condition $u(0,t) = h(t) = t^{3+1/2}$, and (ii) the exact solution $u^{ext}(x,t) = t^{10}[\exp(x^2) + 10\pi]$, in which the boundary condition is given by $u(0,t) = h(t) = 10\pi t^{10}$. We solve the problem by taking $T = L = 1$, setting $\tau = \nu = 1/2$, and keeping $N = 15$ in all simulations. In Table 2, we show the corresponding *p*-refinements for the aforementioned problems, where we achieve an exponential-like convergence in both cases.

We finally conclude the work by comparing the performance of the developed methods with the FDM developed in [25], where the fractional derivative ${}_0\mathcal{D}_t^{\nu} u(t)$ is represented as

$$
{}_0\mathcal{D}_t^{\tau} u(x,t) = \frac{1}{\Gamma(2-\tau)} \sum_{j=0}^{k} a_j \frac{u(x,t_{k+1-j}) - u(x,t_{k-j})}{(\Delta t)^{\tau}} + r_{\Delta t}^{k+1},
\tag{6.2}
$$

TABLE 3

CPU time (seconds) on a dual-core 2.9-GHz Intel processor, corresponding to PG-SM, PG-DSEM, and FDM with $\nu = 1/2$ (kept constant), when the exact solution is $u(x,t) = t^3x^3$. In all cases, we set spatial polynomials order $M = 3$, and we set $\Omega = [0,1] \times [0,1]$.

$\tau = 1/10$

Error	SM-DSEM	DSEM-DSEM($N_{el}^x = N_{el}^t = 2$)	FDM($N_g^t = 200$)
$\mathcal{O}(10^{-4})$	3.69	–	($N_g^x = 10$) 15.705
$\mathcal{O}(10^{-5})$	4.69	(exact) 4.09	($N_g^x = 40$) 173.385

$\tau = 1/2$

Error	SM-DSEM	DSEM-DSEM($N_{el}^x = N_{el}^t = 2$)	FDM($N_g^t = 200$)
$\mathcal{O}(10^{-4})$	3.64	–	($N_g^x = 50$) 253.771
$\mathcal{O}(10^{-5})$	4.58	(exact) 4.01	($N_g^x = 300$) 12128.341

$\tau = 9/10$

Error	SM-DSEM	DSEM-DSEM($N_{el}^x = N_{el}^t = 2$)	FDM($N_g^t = 200$)
$\mathcal{O}(10^{-4})$	3.60	–	($N_g^x = 500$) $5.89 \cdot 10^4$
$\mathcal{O}(10^{-5})$	4.55	(exact) 4.13	($N_g^x = 2000$) Out of Memory

where $r_{\Delta t}^{k+1} \le C_u(\Delta t)^{2-\tau}$ and $a_j := (j+1)^{1-\tau} - j^{1-\tau}$, $j = 0, 1, \ldots, k$, and where a similar formulation can be obtained for the spatial fractional derivative as

$$ {}_0\mathcal{D}_x^{\nu} u(x,t) = \frac{1}{\Gamma(2-\nu)} \sum_{j=0}^{k} b_j \frac{u(x, t_{k+1-j}) - u(x, t_{k-j})}{(\Delta x)^{\nu}} + r_{\Delta x}^{k+1}, \tag{6.3} $$

where $b_j := (j+1)^{1-\nu} - j^{1-\nu}$, $j = 0, 1, \ldots, k$.

In Table 3, we compute the CPU time (in seconds), required for solving (2.1), corresponding to three temporal fractional orders $\tau = 1/10$, $1/2$, and $9/10$, where we keep the spatial fractional order $\nu = 1/10$ fixed. Here, the exact solution is $u(x,t) = t^3x^3$ and the integration time $T = 1$ and the spatial domain size $L = 1$. We compare SM-DSEM with ($N_{el} = 1$) and ($N_{el} = 2$) elements with FDM.

We first observe that our schemes are not sensitive to the fractional order τ; however, the CPU time in FDM is shown to be strongly dependent on τ. It is actually consistent with the fact that the order of accuracy of FDM is $\mathcal{O}((\Delta t)^{2-\tau} + (\Delta x)^{2-\nu})$. Here, we set the relatively big error-levels $\mathcal{O}(10^{-4})$ and $\mathcal{O}(10^{-5})$ for comparison, and the spatial fractional order $\nu = 1/2$ was kept constant. We observe that when τ is very small, FDM and our methods become comparable in terms of computational cost. However, increasing τ to $1/2$ and $9/10$, the cost of FDM becomes *two to four orders of magnitude* greater than that in our methods, depending on the error level and τ. Moreover, we observe that when τ is close to one, FDM becomes almost first-order accurate in time, which leads to a significant amount of memory storage that might not be available on a PC. Clearly, for higher values of ν, even larger memory allocation is required; moreover, the CPU time will significantly be increased in FDM. Regarding DSEM-DSEM and for all the aforementioned cases, we obtain the *exact* solution by setting $N = M = 3$.

Appendix A. Derivation of SM-DSEM scheme. We partition the computational domain into N_{el} nonoverlapping space-time elements, $\Omega_e = [x_{e-1/2}, x_{e+1/2}] \times [0, T]$. Next, we test the TSFAE (2) against some proper test function $v^e(x,t)$, then integrate over the subdomain Ω_e, and using Lemma 3.4 to carry out the temporal fractional integration-by-parts, we obtain

(A.1)
$$\Big({}_0\mathcal{D}_t^{\tau/2} u(x,t),\, {}_t\mathcal{D}_T^{\tau/2} v^e(x,t) \Big)_{\Omega_e} + \theta \Big({}_0\mathcal{D}_x^{\nu} u(x,t),\, v^e(x,t) \Big)_{\Omega_e} = \Big(f(x,t), v^e(x,t) \Big)_{\Omega_e}.$$

Due to our domain-decomposition, and the definition of the spatial fractional derivative with lower terminal beginning at $x = 0$, we obtain an equivalent yet more efficient expression as follows:

$$\begin{aligned}(A.2)\quad \Big({}_0\mathcal{D}_x^{\nu} u(x,t),\, v^e(x,t) \Big)_{\Omega_e} &= \Big(\frac{1}{\Gamma(1-\nu)} \frac{\partial}{\partial x} \int_{x^+_{e-1/2}}^{x} \frac{u(z,t)\,dz}{(x-z)^{\nu}},\, v^e(x,t) \Big)_{\Omega_e} \\ &+ \Big(\frac{1}{\Gamma(1-\nu)} \frac{\partial}{\partial x} \int_{x^-_{e-1/2}}^{x^+_{e-1/2}} \frac{u(z,t)\,dz}{(x-z)^{\nu}},\, v^e(x,t) \Big)_{\Omega_e} \\ &+ \Big(\frac{1}{\Gamma(1-\nu)} \frac{\partial}{\partial x} \int_{0}^{x^-_{e-1/2}} \frac{u(z,t)\,dz}{(x-z)^{\nu}},\, v^e(x,t) \Big)_{\Omega_e},\end{aligned}$$

where we can rewrite (A.2) as

(A.3)
$$\begin{aligned}\Big({}_0\mathcal{D}_x^{\nu} u(x,t)\,,\, v^e(x,t) \Big)_{\Omega_e} &= \Big({}_{x^+_{e-1/2}}\mathcal{D}_x^{\nu} u(x,t),\, v^e(x,t) \Big)_{\Omega_e} \\ &+ \left(\frac{1}{\Gamma(1-\nu)} \frac{\partial}{\partial x} \int_{x^-_{e-1/2}}^{x^+_{e-1/2}} \frac{u(z,t)\,dz}{(x-z)^{\nu}},\, v^e(x,t) \right)_{\Omega_e} + \mathcal{H}_e^x,\end{aligned}$$

where the middle term can be obtained as

$$\begin{aligned}(A.4)\qquad &\left(\frac{1}{\Gamma(1-\nu)} \frac{\partial}{\partial x} \int_{x^-_{e-1/2}}^{x^+_{e-1/2}} \frac{u(z,t)\,dz}{(x-z)^{\nu}},\, v^e(x,t) \right)_{\Omega_e} \\ &\approx - \int_0^T \frac{v^e(x^-_{e+1/2},t)(\Delta x_e)^{1-\nu}}{(1-\nu)\Gamma(1-\nu)} [\![u(x_{e-1/2},t)]\!]\, dt,\end{aligned}$$

where $(\Delta x_e)^{1-\nu} = (x_{e+1/2} - x_{e-1/2})^{1-\nu}$ and $[\![u(x_{e-1/2},t)]\!]$ denotes the jump discontinuity in the solution across the interface between elements Ω_e and I_{e-1} along the time-axis at $x = x_{e-1/2}$. We also obtain the history-load term H_e^x as

$$(A.5)\qquad \mathcal{H}_e^x = \frac{1}{\Gamma(1-\nu)} \left(\sum_{\varepsilon=0}^{e-1} \frac{\partial}{\partial x} \int_{I_\varepsilon} \frac{u^\varepsilon(x,z)dz}{(x-z)^{\nu}}, v^e(x,t) \right)_{\Omega_e}.$$

Plugging (A.5), (A.4) into (A.3), then plugging (A.3) into (A.1) after carrying out the spatial fractional integration-by-parts using Lemma 3.5, we obtain

$$\begin{aligned}(A.6)\quad &\Big({}_0\mathcal{D}_t^{\tau/2} u(x,t),\, {}_t\mathcal{D}_T^{\tau/2} v^e(x,t) \Big)_{\Omega_e} + \theta \left({}_{x^+_{e-1/2}}\mathcal{D}_x^{\nu/2} u(x,t),\, {}_x\mathcal{D}^{\nu/2}_{x^-_{e+1/2}} v^e(x,t) \right)_{\Omega_e} \\ &\quad - \frac{\theta(\Delta x)_e^{1-\nu}}{(1-\nu)\Gamma(1-\nu)} \int_0^T v^e(x^-_{e+1/2},t)\, [\![u^e(x_{e-1/2},t)]\!] dt + \mathcal{H}_e^x \\ &= \Big(f(x,t), v^e(x,t) \Big)_{\Omega_e}.\end{aligned}$$

The variational (weak) form (A.6) is an infinite-dimensional problem. Seeking the solution in each subdomain Ω_e of the form

$$u_{MN}(x,t) = \sum_{m=0}^{M}\sum_{n=1}^{N} \hat{u}_{mn}\tilde{P}_m^{\eta,0}(x^e)\ {}^{(1)}\tilde{\mathcal{P}}_n^{\mu}(t),$$

as a linear combination of elements in the basis function space V^e, and plugging it into (A.6), we obtain the variational form (3.21). At last, we need to provide a more efficient expression for the history-load term $\mathcal{H}_e^x$ in (A.5):

$$\mathcal{H}_e^x = \sum_{m,n}\sum_{\varepsilon=1}^{e-1}(M_t)_{jn}\frac{1}{\Gamma(1-\nu)}\Bigg(\int_{x_{\varepsilon-1/2}}^{x_{\varepsilon+1/2}}\frac{\hat{u}_{mn}^{\varepsilon}\tilde{P}_m^{\eta,0}(s)\ ds}{(x-s)^{\nu}}\tilde{P}_i^{0,\chi}(x)\Big|_{x=x_{e+1/2}^{-}}^{x=x_{e-1/2}^{+}} - \int_{x_{e-1/2}}^{x_{e+1/2}}\int_{x_{\varepsilon-1/2}}^{x_{\varepsilon+1/2}}\frac{\hat{u}_{mn}^{\varepsilon}\tilde{P}_m^{\eta,0}(s)\ ds}{(x-s)^{\nu}}\frac{d}{dx}\tilde{P}_i^{0,\chi}(x)dx\Bigg).$$

Since $\tilde{P}_m^{\eta,0}(s)$ are at most of degree M in each element Ω_e, we can carry out integration-by-parts M recursive times to eliminate the double integral. It leads to the history term shown in (3.32), where we reduce the calculation of the history term to a function evaluation and a one-dimensional integration carried out in the current element Ω_e. Finally, we obtain the history-load term $\mathcal{H}_e^x$ in a computationally efficient form as

$$(\mathcal{H}_e^x)_{ij} = \theta\sum_{m,n}\hat{u}_{mn}(M_t)_{jn}\left(F_e(x)P_i^{0,\nu/2}(x)\Big|_{x=x_{e-1/2}^{+}}^{x=x_{e+1/2}^{-}} - \int_{x_{e-1/2}}^{x_{e+1/2}}F_e(x)\frac{d}{dx}P_i^{0,\nu/2}(x)\ dx\right),$$

in which $F_e(x)$ represents the history function associated with the current element Ω_e

$$F_e(x) = \sum_{\varepsilon=1}^{e-1}F_e^{\varepsilon}(x)$$

consisting of all the past element contributions as

$$F_e^{\varepsilon}(x) = \sum_{m}\hat{u}_{mn}^{\varepsilon}\sum_{\delta=0}^{M}\tau_{\delta}(x-s)^{\delta+1-\nu}\tilde{P}_m^{\eta,0(\delta)}(s)\Big|_{s=s_{\varepsilon-1/2}^{+}}^{s=s_{\varepsilon+1/2}^{-}}, \tag{A.7}$$

where $\tilde{P}_m^{\eta,0(\delta)}(s)$ represents the δth derivative of $\tilde{P}_m^{\eta,0}(s)$; moreover, the coefficient $\tau_{\delta} = -1/\{\Gamma(1-\nu)\prod_{m=0}^{\delta}(m+1-\nu)\}$ decays in a factorial fashion with respect to δ.

Acknowledgment. The authors would like to thank Mr. Ian Alevy for the helpful collaboration during his short visit at the CRUNCH group.

REFERENCES

[1] R. Askey and J. Fitch, *Integral representations for Jacobi polynomials and some applications*, J. Math. Anal. Appl., 26 (1969), pp. 411–437.
[2] E. Barkai, R. Metzler, and J. Klafter, *From continuous time random walks to the fractional Fokker-Planck equation*, Phys. Rev. E, 61 (2000), 132.
[3] L. Blank, *Numerical Treatment of Differential Equations of Fractional Order*, Citeseer, 1996.
[4] J. Cao and C. Xu, *A high order schema for the numerical solution of the fractional ordinary differential equations*, J. Comput. Phys., 238 (2013), pp. 154–168.

[5] A. R. Carella, *Spectral Finite Element Methods for solving Fractional Differential Equations with applications in Anomalous Transport*, Ph.D. thesis, Norwegian University of Science and Technology, 2012.
[6] A. Carpinteri and F. Mainardi, *Fractals and Fractional Calculus in Continum Mechanics*, Springer-Verlag, Berlin, 1998.
[7] W. Chester, *Resonant oscillations in closed tubes*, J. Fluid Mech., 18 (1964), pp. 44–64.
[8] W. H. Deng and J. S. Hesthaven, *Local discontinuous Galerkin methods for fractional diffusion equations*, ESAIM: Math. Model. Numer. Anal., 47 (2013), pp. 1845–1864.
[9] K. Diethelm and N. J. Ford, *Analysis of fractional differential equations*, J. Math. Anal. Appl., 265 (2002), pp. 229–248.
[10] G. J. Fix and J. P. Roop, *Least squares finite-element solution of a fractional order two-point boundary value problem*, Comput. Math. Appl., 48 (2004), pp. 1017–1033.
[11] B. Gustafsson, H. O. Kreiss, and J. Oliger, *Time-Dependent Problems and Difference Methods*, Pure and Appl. Methods 67, Jhon Wiley, New York, 1995.
[12] E. Hanert, *A comparison of three Eulerian numerical methods for fractional-order transport models*, Environ. Fluid Mech., 10 (2010), pp. 7–20.
[13] B. Henry and S. Wearne, *Fractional reaction-diffusion*, Phys. A, 276 (2000), pp. 448–455.
[14] J. S. Hesthaven, S. Gottlieb, and D. Gottlieb, *Spectral Methods for Time-Dependent Problems*, Cambridge Moriogr. Appl. Comput. Math. 21, Cambridge University Press, Cambridge, UK, 2007.
[15] I. M. Jaimoukha and E. Kasenally, *Krylov subspace methods for solving large Lyapunov equations*, SIAM J. Numer. Anal., 31 (1994), pp. 227–251.
[16] G. E. Karniadakis and S. J. Sherwin, *Spectral/hp Element Methods for CFD*, 2nd ed., Oxford University Press, New York, 2005.
[17] J. J. Keller, *Propagation of simple non-linear waves in gas filled tubes with friction*, Z. Angew. Math. Phys., 32 (1981), pp. 170–181.
[18] M. M. Khader, *On the numerical solutions for the fractional diffusion equation*, Commun. Nonlinear Sci. Numer. Simul., 16 (2011), pp. 2535–2542.
[19] M. M. Khader and A. S. Hendy, *The approximate and exact solutions of the fractional-order delay differential equations using Legendre pseudospectral method*, Internat. J. Pure Appl. Math., 74 (2012), pp. 287–297.
[20] V. V. Kulish and J. L. Lage, *Application of fractional calculus to fluid mechanics*, J. Fluids Engrg., 124 (2002), pp. 803–806.
[21] T. Langlands and B. Henry, *The accuracy and stability of an implicit solution method for the fractional diffusion equation*, J. Comput. Phys., 205 (2005), pp. 719–736.
[22] R. J. LeVeque, *Finite Volume Methods for Hyperbolic Problems*, Cambridge Texts Appl. Math. 31, Cambridge University Press, Cambridge, UK, 2002.
[23] X. Li and C. Xu, *A space-time spectral method for the time fractional diffusion equation*, SIAM J. Numer. Anal., 47 (2009), pp. 2108–2131.
[24] X. Li and C. Xu, *Existence and uniqueness of the weak solution of the space-time fractional diffusion equation and a spectral method approximation*, Commun. Comput. Phys., 8 (2010), pp. 1016–1051.
[25] Y. Lin and C. Xu, *Finite difference/spectral approximations for the time-fractional diffusion equation*, J. Comput. Phys., 225 (2007), pp. 1533–1552.
[26] W. McLean and K. Mustapha, *Convergence analysis of a discontinuous Galerkin method for a sub-diffusion equation*, Numer. Algorithms, 52 (2009), pp. 69–88.
[27] M. M. Meerschaert and A. Sikorskii, *Stochastic Models for Fractional Calculus*, de Gruyter Stud. Math. 43 de Gruyter, Berlin, 2012.
[28] K. S. Miller and B. Ross, *An Introduction to the Fractional Calculus and Fractional Differential Equations*, John Wiley, New York, 1993.
[29] T. Penzl, *A cyclic low-rank Smith method for large sparse Lyapunov equations*, SIAM J. Sci. Comput., 21 (1999), pp. 1401–1418.
[30] I. Podlubny, *Fractional Differential Equations*, Academic Press, San Diego, CA, 1999.
[31] E. A. Rawashdeh, *Numerical solution of fractional integro-differential equations by collocation method*, Appl. Math. Comput., 176 (2006), pp. 1–6.
[32] W. H. Reed and T. R. Hill, *Triangular Mesh Methods for the Neutron Transport Equation*, Report LA-UR-73-479, Los Alamos National Laboratory, Los Alamos, NM, 1973.
[33] J. P. Roop, *Computational aspects of FEM approximation of fractional advection dispersion equations on bounded domains in r2*, J. Comput. Appl. Math., 193 (2006), pp. 243–268.
[34] Y. Saad, *Numerical Solution of Large Lyapunov Equations*, Research Institute for Advanced Computer Science, NASA Ames Research Center, 1989.

[35] N. Sugimoto, *Burgers equation with a fractional derivative: Hereditary effects on nonlinear acoustic waves*, J. Fluid Mech, 225 (1991), pp. 631–653.
[36] N. Sugimoto and T. Kakutani, *Generalized Burgers' equation for nonlinear viscoelastic waves*, Wave Motion, 7 (1985), pp. 447–458.
[37] Z. Sun and X. Wu, *A fully discrete difference scheme for a diffusion-wave system*, Appl. Numer. Math., 56 (2006), pp. 193–209.
[38] E. L. Wachspress, *Iterative solution of the Lyapunov matrix equation*, Appl. Math. Lett., 1 (1988), pp. 87–90.
[39] Q. Xu and J. S. Hesthaven, *Discontinuous Galerkin Method for Fractional Convection-Diffusion Equations*, arXiv:1304.6047, 2013.
[40] M. Zayernouri and G. E. Karniadakis, *Fractional Sturm-Liouville eigen-problems: Theory and numerical approximations*, J. Comput. Phys., 47 (2013), pp. 2108–2131.
[41] M. Zayernouri and G. E. Karniadakis, *Exponentially accurate spectral and spectral element methods for fractional ODEs*, J. Comput. Phys., 257 (2014), pp. 460–480.
[42] M. Zayernouri and G. E. Karniadakis, *Fractional spectral collocation method*, SIAM J. Sci. Comput., 36 (2014), pp. A40–A62.
[43] O. C. Zienkiewicz, R. L. Taylor, and J. Z. Zhu, *The Finite Element Method: Its Basis and Fundamentals*, Butterworth-Heinemann, London, 2005.